NUMERICAL SIMULATIONS ON OXY-MILD COMBUSTION OF PULVERIZED COAL IN AN INDUSTRIAL BOILER

Diego Perrone[1], Teresa Castiglione[1*], Adam Klimanek[2], Pietropaolo Morrone[1], Mario Amelio[1]

[1]Department of Mechanical, Energy and Management Engineering-DIMEG, University of Calabria, Ponte Bucci, Cubo 44 C, 87036 Rende, Italy
[2] Institute of Thermal Technology, Silesian University of Technology, Konarskiego 22, 44-100 Gliwice, Poland

Abstract

The purpose of this study is to analyze the possibility of combining two innovative combustion technologies in large-scale pulverized coal fired plants: Moderate or Intense Low Oxygen Dilution (MILD) and Oxy-Combustion. The combination of both technologies, namely Oxy-MILD combustion, is expected to bring synergetic effects: NO_x reduction, CO_2 capture possibility, fuel flexibility and uniformity of heat fluxes and species concentrations. In this work, the predictable advantages of adopting this technology, with respect to conventional boilers, are evaluated by means of CFD modelling, in terms of pollutant emissions and uniformity of heat fluxes. In a previous work, the developed CFD model was validated against available experimental data of MILD combustion in a pilot-scale furnace and it was demonstrated that the proposed model captures the combustion features with good accuracy. In order to identify the effective potential of Oxy-MILD combustion and its possible uses on an industrial scale, an application in the boiler is analyzed in the current work. Results show that the temperature and species concentration distributions reach an acceptable level of uniformity in the boiler; similarly, the wall heat flux profile is uniform along the boiler height, as in the fluidized bed technology. The CO_2 concentration at the boiler exit, for an excess oxygen ratio of 1.1, is about 95.8%; this value is slightly increased for lower excess oxygen ratio, even though in this case, incomplete combustion occurs. Finally, lower NO_x (70 mg/MJ) than other technological solutions are obtained owing to the prevention of thermal and prompt NO_x, owing to the absence of N_2 in the oxidizer, and to the re-burning mechanism, which is predominant especially when recycled NO_x is considered.

Keywords: Pulverized coal firing, MILD combustion, Oxy combustion, Industrial boiler, NO_x, CO_2.

LIST OF SYMBOLS

a	absorption coefficient [m^{-1}]
A	surface area [m^2]; pre-exponential factor [kg/m^2 s Pa]
c_0	initial fraction of bridges in coal lattice [-]
c_i	empirical coefficients in Gennetti correlation [-]
c_p	specific heat capacity [J/mol K]
C	linear-anisotropic phase function coefficient [-]
$\mathcal{D}$	effective diffusion coefficient [m^2/s]
E_p	particle equivalent emission [W/m^3]
F_D	drag coefficient [-]
g	gravity [9.81 m/s^2]
G	incident radiation [W/m^2]
h	heat transfer coefficient [W/m^2 K], enthalpy [J/kg]
J	diffusion flux [kg /m^2s]
m	mass [kg]
n	refractive index [-]
M	molecular weight [kg/kmol]
p	partial pressure [Pa]
q	heat flux vector [W/m^2]
Q_{sr}	specific heat of reaction due to particle surface reaction [J/kg]
R	reaction rate [kg/m^3 s]
S_h	source term for energy exchange [W/m^3]
S_i	source term for mass of species *i* [kg/m^3 s]

S_m	source term for mass exchange [kg/m^{3}s]
S_{mom}	source term for momentum exchange [kg/m^{2}s^2]
S_{HCN}	source term for HCN transport equation [kg/m^3 s]
S_{NO}	source term for NO transport equation [kg/m^3 s]
t	time [s]
T	temperature [K]
v	velocity vector [m/s]
V	volume [m^3]
x	position vector [m]
Y	mass fraction [-]

Greek symbols

ϵ	emissivity [-]
Γ	diffusivity [m]
ρ	density [kg/m^3]
σ	Stefan-Boltzmann constant [W/m^2 K^4]
σ_s	Scattering coefficient [m^{-1}]
τ	Stress tensor [kg/m^{2}s^2]
θ	radiation temperature [K]

Subscripts

f	fluid
i	index
j	index
p	particle

Abbreviations

^{13}C NMR	Carbon-13 Nuclear Magnetic Resonance
CFD	Computational Fluid Dynamics
CDC	Colorless Distributed Combustion
CPD	Chemical Percolation Devolatilization
EDM	Eddy Dissipation Model
FLOX	Flameless Oxidation
FRM	Finite Rate Model
HTAC	Highly Preheated Air Combustion
IFRF	International Flame Research Foundation
MILD	Moderate or Intense Low Oxygen Dilution
PC	Pulverized Coal
PISO	Pressure-Implicit with Splitting of Operators
RTE	Radiative Transfer Equation
RFG	Recirculated Flue Gas

1. INTRODUCTION

Safeguarding the environment is nowadays the most important target for energy production all over the world. Solutions based on renewable sources are widespread. Despite this, coal contributed to nearly half of the increase in global energy use over the past decade [1, 2, 3] and still constitutes the most used fuel for energy production owing to its abundant reserves and low price. It is well known, however, that coal presents environmental issues related both to pollutant emissions, such as nitrogen oxide (NO_x) and sulfur oxide (SO_x), and to the Greenhouse Gas (GHG) emissions (CO_2), which are responsible for climate change.

Several technological solutions were proposed for reducing CO_2 emissions from coal-fired power plants; among them: pre-combustion capture, post-combustion capture and Oxy-fuel

combustion. A recent study [4] compared these three technologies and concluded that Oxy-combustion is the most competitive one, both in terms of energy efficiency and economic performance, especially for retrofitting existing coal-fired power plants. This technology significantly modifies the combustion process: Oxy-fuel combustion is based, in fact, on the removal of nitrogen from the oxidizer to carry out combustion in oxygen or in a mixture of O_2 and recycled flue gas. The removal of nitrogen from the oxidizer generates a high CO_2 concentration stream at the end of the combustion process, which is ready for sequestration, after removing water vapor and other impurities. Typically, recycled flue gas is used to replace nitrogen and to control the flame temperature to within the acceptable limits of the boiler materials. In this case, the combustion process takes place in an O_2/CO_2-rich atmosphere and the temperatures ranges are similar to those for combustion in air.

The application of oxy-fuel combustion to coal-fired power plants for the control of CO_2 emissions was first proposed in the early ’80s by [5-7]. Since then, owing to the foreseen benefits of this technology, an intense research activity on the oxy-fuel fundamentals was carried out in various institutions, which contributed considerably to the understanding of this process through experimental test facilities [8-18] and by means of Computational Fluid Dynamics (CFD). CFD applications have been abundant recently and studies were carried out on oxy-combustion on the lab and pilot scale with the main purpose to develop and validate sub-models for the new combustion environment. The most important differences with modeling in air, in particular, concern the radiative heat transfer, where the absorption coefficient is a function of the environment gas composition, temperature and pressure; the heterogeneous reactions kinetics of char oxidation and gasification reactions are slower in a CO_2 rich atmosphere and the species are burned in a stream which is different from conventional air-fuel combustion. Among the most recent studies, Hu et al. [19] modeled oxy-combustion in a 0.5 MW test facility, with focus on the absorption coefficient and radiation intensity models; Álvarez et al. [20,21] proposed and validated a model for coal devolatilization under oxy combustion in an entrained flow reactor by the use of CFD; Hu et al. [22] investigated the flame profile and the heat transferred through walls in both large scale air-coal combustion boiler and large scale oxy-coal combustion boiler and provides useful guidelines of operation conditions to design oxy-coal combustion boilers. A review of the current status can be found in Toftegaard et al. [15] and Chen et al. [4].

Another advantage related to this combustion technology is the contribution to NO_x

reduction in comparison to air-firing. The effects of CO_2 concentrations on the NO_x emissions in coal combustion with recycled CO_2 was performed by Okazaki and Ando [23]. They obtained an NO_x reduction amounting to less than one third by adopting the O_2/CO_2 combustion system with respect to combustion in air. Ikeda et al. [24] carried out experimental investigations on NO_x emissions from an Oxy-coal pilot plant. They demonstrated that NO_x emissions in O_2/CO_2 are about 20% lower than in air mode. A more important reduction, by about 50%, was obtained in O_2/RFG mode, owing to the NO_x contained in the recirculated flue gas (RFG), supplied by a secondary stream to the flame.

Despite Oxy-combustion being accepted as a competitive carbon capture technology, it is still in the early stages of its development and several issues still remain unresolved; from a technological point of view, these concern system integration and optimization, optimal combustor and burner design, industrial-scale demonstration of the oxy-coal combustion in order to verify the observations and theories developed from lab and bench scale studies [4,15]. From the modeling side, the development and validation of more accurate sub-models are still needed, especially for prediction of NO_x formation levels. Furthermore, extensive applications of CFD are expected in the scale-up of oxy-coal combustion facilities.

In recent years, a new combustion technology has been developed for pulverized coal boilers [25-27], namely Moderate or Intense Low Oxygen Dilution (MILD) combustion. For the sake of clarity, this technology is also known as HiTAC (highly preheated air combustion) [28], FLOX (flameless oxidation) [29] or CDC (colorless distributed combustion) [30]. Despite these terms not being identical, the combustion characteristics are very similar to each other in terms of uniformity of temperature distribution and significant low NO_x emissions; hence, the terms will be considered interchangeable throughout the paper.

MILD combustion exploits the initial preheating of combustion air up to 800÷1300 °C and the simultaneous recirculation of the hot flue gas. This recirculation causes dilution of the combustion air stream and the fuel stream before the ignition occurs. In this way, a uniform distribution of temperature and of chemical species is obtained and the temperature peaks are avoided. Consequently, MILD technology allows low NO_x and CO emissions and high and uniform heat fluxes. The latter aspect is particularly favorable in boilers, which adopt the once-through tubes for water circulation like the ones typically used in supercritical and ultra-supercritical steam cycle plants. Recent studies [31,32] have demonstrated, however, that air preheating is not necessary for obtaining MILD conditions; on the contrary, the fundamental

feature is to inject air with high momentum in order to get significant flue gas entrainment and oxidizer dilution. This allows the MILD technology applicable to coal fired boilers. The application of MILD technology to pulverized coal requires, however, the design of new combustion chambers. Several studies were carried out in order to improve the performance of the MILD technology to pulverized coal and to optimize the combustion chamber design. The International Flame Research Foundation (IFRF) carried out experiments on an 880kW furnace using solid, gaseous and liquid fuels [33,34]. Afterwards, Suda et al. [35] investigated the NO_x emissions, char burnout, flame stability and ignition delay in a 250 kW furnace. They observed that the temperature peak remains constant in a range of temperatures of preheated air. Ristic et al. [36,37] obtained experimental and numerical results by carrying out measurements and simulations in a pilot furnace. Schaffel et al. [27] proposed a numerical modelling for pulverized coal combustion in pre-heated air condition in a pilot IFRF furnace and their findings revealed a good agreement with the experimental results; subsequently, Schaffel et al. [38] proposed a new concept of boiler for pulverized coal, designed for supercritical operations, which is equipped with five burners, enforces a very high momentum of the combustion air stream and provides an intensive in-furnace recirculation. Perrone et al. [39], by means of numerical simulation, observed that the distance between the fuel and oxidizer jets plays an important role in order to obtain the "mildness" condition. When this distance increases, the oxygen concentration decreases, therefore the NO_x emissions decrease. A CFD study was presented in order to improve the boiler design and the study demonstrated that MILD technology can be an efficiently used for pulverized coal fired boilers.

The idea of combining the MILD and Oxy-fuel combustion and achieving, therefore, the benefits of both techniques was recently proposed [40-42]. This technology is expected to improve the performance of oxy-coal combustion in terms of higher energy efficiency, better environmental performance and lower cost; therefore it is worth to be explored. As for oxy-fuel combustion, several issues need to be addressed for this technology at its conceptual stage. The use of CFD, in such a case, is a very useful tool in order to explore the optimal organization of the flow and mixing patterns within the chamber. A number of numerical studies on Oxy-MILD combustion, related to small-scale systems, were carried out. Li et al. [43] presented a study of MILD oxy-combustion for gaseous fuels and evaluated the effects of the equivalence ratio on MILD conditions. Furthermore, they focused on the NO formation mechanism and found that N_2O-intermediate route plays a crucial role in forming NO, with respect to thermal, prompt and

NNH routes. Li et al. [44] experimentally investigated the global characteristics of both MILD oxy-combustion and air combustion of firing light oil and pulverized coal in a pilot-scale furnace, for various burner configurations. The most important findings show that, for MILD combustion, NO emissions are reduced much more effectively in the oxy-combustion case than in the air combustion case. Tu et al. [45] carried out a numerical study for a cuboid small chamber with two oxygen nozzles and a central fuel nozzle. They focused on O_2 concentrations in the flue gases. Liu et al. [46] investigated the spacing of O_2 nozzles and CO_2 jet and the ignition delay for a small pilot cylindrical chamber by the use of CFD. Hu et al. [47] proposed an optimization of the global reaction mechanism for MILD oxy-combustion of methane. The study was carried out by using both computational fluid dynamics (CFD) simulations and experimental validation in a laboratory-scale furnace. The proposed optimized global mechanism significantly improves the prediction of temperatures, equilibrium concentrations of major species and the peak CO concentration for the MILD oxy-combustion, in comparison to other global mechanisms. All these studies are, however, concerned on small pilot-scale installations and no large-scale applications have been explored, to the best of the authors' knowledge.

The purpose of the present work is to contribute to the research on Oxy-MILD combustion in pulverized coal firing, with particular regard to large scale boilers. In this work, the Oxy-MILD combustion in a large-scale boiler will be analyzed referring to the new conceptual boiler presented by [38]. Specifically, a quantitative analysis of temperature distribution, wall heat fluxes and species concentrations will be presented and compared to other technological solutions. The possibility of using low excess oxygen ratios is also investigated by analyzing three different cases. This paper follows a preliminary work [48], which focused on the optimal location of the oxygen and fuel nozzles and configured the chamber geometry in order to improve the momentum of the oxidizer and fuel jets. In the present paper, a different burner geometry will be analyzed with respect to [48] and differently from [48], user defined functions for modeling the radiative heat transfer in O_2/CO_2 atmosphere will be implemented. Finally, results for NO_x emission will be widely discussed.

The technological feasibility of Oxy-MILD combustion, from a global point of view, must be carefully evaluated in terms of total energy consumption and costs. The adoption of this technology in existing or in newly-built PC plants requires, in fact, the integration of several components (air separation unit, carbon dioxide purification, compression and liquefaction, flue

gas recycle system, etc.), which severely affect the efficiency of the whole plant. Despite these aspects being of fundamental importance, the focus of the present paper relies on the basic features of the combustion process and on combustion products; the technical/economic aspects will not be, therefore, taken into consideration in the current paper.

2. MODEL DESCRIPTION

The proposed study regards the analysis of a new industrial boiler fueled with pulverized coal under oxy-MILD combustion conditions. The coal injection into the boiler is realized by means of a CO_2 stream, through a central jet. The oxidizer, formed by O_2/CO_2 mixture, is injected into the boiler through a number of jets surrounding the central one. The present work focuses on the combustion process inside the boiler; therefore, the external components for the CO_2 and oxygen supply are not taken into consideration.

The modeling of the combustion process is challenging owing to the quite complex mechanisms involving the interaction between the coal particles and the main stream, the mixing with the oxidizer and the burning phase; this last phase, in turn, includes the following steps: heating, devolatilization, volatile combustion and char burnout. The sub-models proposed for each process, which consider combustion under oxy conditions, are implemented in the CFD code FLUENT [49] and are described in this section.

The Eulerian-Lagrangian approach is used to model the Oxy-MILD combustion process, where the coal particles are dispersed in the gas phase. In order to predict flow, temperature and concentration of species, the governing equations of mass, momentum and energy conservation are solved for the gas phase; furthermore, the conservation equation of chemical species when combustion takes place, is added. The equations are summarized below:

-Mass
$$\frac{\partial \rho}{\partial t} + (\nabla \cdot \rho \mathbf{v}) = S_m \tag{1}$$

-Momentum
$$\frac{\partial}{\partial t}(\rho \mathbf{v}) + \nabla \cdot (\rho \mathbf{v}\mathbf{v}) = -\nabla p + \nabla \cdot \boldsymbol{\tau} + \rho \boldsymbol{g} + S_{mom} \tag{2}$$

-Energy
$$\frac{\partial}{\partial t}(\rho \mathrm{h}) + \nabla \cdot (\rho \mathbf{v} h) = \frac{\partial p}{\partial t} + \bar{\boldsymbol{\tau}} : \nabla \mathbf{v} - \nabla \cdot \boldsymbol{q} - \nabla \cdot \left(\sum_i h_i \boldsymbol{J}_i \right) + S_h \tag{3}$$

-Species
$$\frac{\partial}{\partial t}(\rho Y_i) + \nabla \cdot (\rho \mathbf{v} Y_i) = -\nabla \cdot \boldsymbol{J_i} + R_i + S_i \tag{4}$$

In the above equations, ρ is the fluid density, $\mathbf{v}$ is the velocity vector, p is the pressure, $\boldsymbol{\tau}$ is the stress tensor, $\mathbf{g}$ is the vector of gravitational acceleration, h is the enthalpy, $\mathbf{q}$ is the heat flux vector, i is the species index, $\boldsymbol{J}_i$ is the diffusion flux of species i and Y_i is the mass fraction of species i. The terms S_m, S_{mom}, S_h and S_i are the sources due to exchange of mass, momentum, energy and mass of species between the continuous phase and the dispersed phase, respectively. The source term S_h also includes the contribution to the energy equation due to the radiation and the amount of energy released in chemical reactions. Finally, R_i represents the source due to homogeneous and heterogeneous reactions in which species i are produced or consumed.

In addition to the transport equations for the continuous phase, the trajectories of coal particles and the heat and mass transfer to/from them are computed:

-Particles motion
$$\frac{d\mathbf{v}_p}{dt} = F_D\left(\mathbf{v} - \mathbf{v}_\mathrm{p}\right) + \boldsymbol{g}\frac{\left(\rho_p - \rho\right)}{\rho_p} - \frac{\nabla \mathrm{p}}{\rho_p} \quad (5)$$

-Particles trajectory
$$\frac{d\mathbf{x}_p}{dt} = \mathbf{v}_\mathrm{p} \quad (6)$$

-Heat transfer
$$m_p c_p \frac{dT_p}{dt} = hA_p\left(T_f - T_p\right) - f_h\frac{dm_p}{dt}Q_{sr} + A_p\epsilon_p\sigma(\theta_R^4 - T_p^4) \quad (7)$$

-Mass transfer
$$\frac{d\mathrm{m}_p}{dt} = \frac{d\mathrm{m}_{char}}{dt} + \frac{d\mathrm{m}_{vol}}{dt} + \frac{d\mathrm{m}_{water}}{dt} \quad (8)$$

The subscript p refers to particle data, $F_D\left(\mathbf{v} - \mathbf{v}_\mathrm{p}\right)$ is the particle acceleration term due to drag and $-\frac{\nabla \mathrm{p}}{\rho_p}$ is the acceleration due to pressure gradient. In the heat transfer equation, Q_{sr} is the specific heat released due the surface reaction and f_h indicates the fraction of this heat absorbed by the particle during the char combustion process, which, in all simulations, is set to 0.3 [27,48]. The last term indicates the particle radiative heat transfer, where the particle emissivity ϵ_p is set to a constant value of 0.8 [4]. Finally, m_{char}, m_{vol} and m_{water} are the masses of the char, volatiles and water in combustible particle, respectively.

The interaction between phases and in particular the combustion process, are worthy of consideration in the present work and are taken into consideration by the implementation of several sub-models.

2.1 Devolatilization

In the present work, a sub-bituminous coal, whose characteristics are summarized in Table 1 and Table 2 [27], is used. Coal combustion is modeled according to the following steps: heating, devolatilization, volatile combustion and char burnout.

For the devolatilization process, the model adopted in the present work is the Chemical Percolation Devolatilization (CPD) Model [50, 51, 52]. The CPD model requires the definition of several parameters. These are: initial fraction of char bridges (p_0), cluster molecular weight ($M_{w,cl}$), side chain molecular weight ($M_{w,del}$) and lattice coordination number ($\sigma + 1$). The determination of these parameters is quite difficult and usually the ^{13}C NMR spectroscopy is used to obtain the coal structure. Non-linear correlations, better known as Genetti correlations [53], are also available and they allow the estimation of the parameters according to Eq. (9):

$$y = c_1 + c_2 Y_C + c_3 Y_C^2 + c_4 Y_H + c_5 Y_H^2 + c_6 Y_O + c_7 Y_O^2 + c_8 Y_{VM} + c_9 Y_{VM}^2 \qquad (9)$$

where $y = \{M_{w,del}, M_{w,cl}, \sigma + 1, p_0\}$, c_i are empirical coefficients, Y_C, Y_H, Y_O and Y_{VM} are the mass fractions of carbon, hydrogen, oxygen and volatile matter, respectively. Another parameter is the number of stable bridges, c_0, which exist in the parent coal or are formed early in the pyrolysis process for low rank coals. In the CPD model, this parameter is estimated according to the following correlation [53]:

$$\begin{aligned} c_0 = \min[0.36, \max\{(0.118\, Y_C - 10.1), 0.0\}] \\ + \min[0.15, \max\{(0.014 Y_O - 0.175), 0.0\}] \end{aligned} \qquad (10)$$

where Y_C and Y_O are the percentage of carbon and oxygen, respectively, on a dry ash free basis.

2.2 Char combustion

After the volatile component of the coal particle is completely evolved, a surface reaction, which consumes the combustible part of the particle, starts. The char combustion process is modeled using the following reactions:

$$C(s) + O_2 \rightarrow CO_2 \qquad (11)$$

$$C(s) + CO_2 \rightarrow 2CO \qquad (12)$$

where the char gasification process in the presence of CO_2 is considered. This must be taken into account when the coal combustion process in the oxidizer atmosphere with high concentrations of CO_2 is modeled [54].The multiple particle surface model is adopted to calculate the rate of the each individual reaction of the surface species C(s). In this study, the required data for the model were adapted from the work of Toporov et al. [55].

2.3 Volatiles combustion

The combustion of volatiles, for the sub-bituminous coal adopted in the present work, is modeled using two homogeneous equations, which involve the oxidation of the pseudo-specie, representing the volatiles, to CO in the first reaction and of CO to CO_2 in the second one:

$$C_{1.33}H_{4.13}O_{0.50} + 1.44O_2 \rightarrow 1.33CO + 2.07H_2O \quad (13)$$

$$CO + 0.5O_2 \rightarrow CO_2 \quad (14)$$

The rate of the two homogenous reactions is provided by the Finite rate/Eddy Dissipation Model (FRM/EDM), with kinetic rates taken from Toporov et al [56].

2.4 Radiation model

Radiative heat transfer plays an important role in boilers as it is the principal mode of heat transfer; the radiation term is responsible for the source term in the energy balance equation (Eq.3) and for the particle heat balance in Eq.7.

The radiative transfer equation (RTE) for modeling radiation intensity [49] is solved using the P-1 model. The transport equation for the incident radiation, G, is given by:

$$\nabla \cdot (\Gamma \nabla G) = (a + a_P)G - 4\pi\left(an^2\sigma\frac{T^4}{\pi} + E_P\right) \quad (15)$$

where a is the gas absorption coefficient, a_P is the particle absorption coefficient, E_P is the equivalent emission of the particles, which correlates with the particle emissivity, ϵ_p, σ is the Stefan-Boltzmann constant, n is the refractive index of the medium and Γ is defined as:

$$\Gamma = \frac{1}{3(a + a_P + \sigma_P)} \quad (16)$$

σ_S being the particle scattering coefficient. Eq.15 can be directly substituted in the energy equation in order to take into account the radiative heat source.

The total gas emissivity of local gas mixture is often calculated by a weighted sum of gray gases model (WSGGM) in combustion CFD modeling [57], in which the model parameters are based on the radiative properties of air-fired flue gases. However, large differences occur between the characteristics of radiative heat transfer in oxy-combustion and in conventional air combustion, owing to the differences in the flue gas composition. If a CO_2 rich atmosphere is considered, this triatomic gas is not transparent to radiation, contrarily to N_2. Therefore, in oxy combustion, the partial pressures are higher than in air combustion, which significantly increases the absorptivity and emissivity of the flue gases. A new and complete set of weighted sum of gray gases model (WSGGM), which is applicable to computational fluid dynamics (CFD) modeling of both air-fuel and oxy-fuel combustion was derived in [58] and was implemented in the present work by means of a user defined function.

For particles emissivity, different approaches are adopted in the literature. In pulverized coal combustion modeling, constant values for particle emissivity and scattering factor are commonly employed, [21,59-63]. Correlations for conversion-dependent particle emissivity and scattering factor were also developed [64,65], even though much effort is needed to develop more accurate models. In the present work, constant values of particle emissivity ϵ_p=0.9 and scattering coefficient $\sigma_P = 0.6$, as suggested in [66], are adopted. It is worth noting that, differently from gas radiation properties, which in oxy-combustion vary considerably with respect to combustion in air, particle emission gives a similar contribution in both combustion environments, as demonstrated by Andersson [67].

2.5 NO_x predictions

The NO_x are, in general, produced through the occurrence of four mechanisms: thermal, fuel, prompt and by means of N_2O. Since the NO_x concentrations are usually small when compared to other species and they do not affect the flow field variables to a large extent, it is possible to predict the NO_x formation in the so-called post-processing mode of a combustion simulation. A NO_x formation path for MILD combustion in air, which considers all the formation mechanisms, was modelled and validated in [27]. This approach will be adopted in the present work, where, however, only Fuel-NO_x are taken into consideration; in fact, owing to the

absence of nitrogen under oxy-MILD combustion, the thermal NO, prompt-NO and NO obtained from N_2O are negligible [68, 69].

The simplified formation path adopted for fuel NO is reported in Fig.1. This simplified path assumes that nitrogen is distributed in char and volatiles. Specifically, the nitrogen contained in char and in the volatiles is converted to HCN and then oxidized to NO or reduced to N_2. The heterogeneous re-burning of NO on the char surface and the homogenous re-burning due to CH_i hydrocarbon are considered as well.

According to the formation path for Fuel-NO_x, the following reactions are considered:

$$\text{Char-N} \rightarrow \text{HCN} \tag{17}$$

$$\text{Vol-N} \rightarrow \text{HCN} \tag{18}$$

$$\text{HCN}+O_2 \rightarrow \text{NO}+\ldots \tag{19.a}$$

$$\text{HCN}+\text{NO} \rightarrow N_2+\ldots \tag{19.b}$$

$$\text{NO}+CH_i \rightarrow \text{HCN}+\ldots \tag{20}$$

$$\text{NO}+\text{Char} \rightarrow N_2+\ldots \tag{21}$$

In order to evaluate the NO_x concentrations, two transport equations are solved:

$$\frac{\partial}{\partial t}(\rho Y_{NO}) + \nabla \cdot (\rho \vec{v} Y_{NO}) = \nabla \cdot (\rho D \nabla Y_{NO}) + S_{NO} \tag{22}$$

$$\frac{\partial}{\partial t}(\rho Y_{HCN}) + \nabla \cdot (\rho \vec{v} Y_{HCN}) = \nabla \cdot (\rho D \nabla Y_{HCN}) + S_{HCN} \tag{23}$$

The HCN source term in Eq. (23) is given by:

$$S_{HCN} = S_{HCN,vol} + S_{HCN,char} - \left(r_{HCN_1} + r_{HCN_2}\right) M_{HCN} 10^{-3} \tag{24}$$

where the constants for the reaction rates r_{HCN_1} and r_{HCN_2}, expressed in $\left(\frac{mole}{m^3} s\right)$, are taken from DeSoete [70]. The sources of HCN from volatiles and from char are determined as follows:

$$S_{HCN,vol} = \frac{\dot{m}_{vol} Y_{N,vol} M_{HCN}}{M_N V} \tag{25}$$

$$S_{HCN,char} = \frac{\dot{m}_{char} Y_{N,char} M_{HCN}}{M_N V} \tag{26}$$

where $\dot{m}_{vol}$, computed by the CPD model, is the rate of volatile matter (in kg/s) and $\dot{m}_{char}$, computed by multiple surface reaction model, is the combustion rate of char in (kg/s). The NO source term from fuel nitrogen is given by the following expression:

$$S_{NO} = S_{NO,coal} + S_{NO,reburn} \tag{27}$$

where the contribution from coal is:

$$S_{NO,coal} = \left(r_{HCN_1} - r_{HCN_2}\right) M_{NO} 10^{-3} \tag{28}$$

while the source term from the re-burning path takes into account both homogeneous and heterogeneous contributions:

$$S_{NO,rebur} = S_{NO,hom,rebur} + S_{NO,het,rebur} \tag{29}$$

The $S_{NO,het,rebur}$ is the source term due to the heterogeneous reduction of NO on the char surface:

$$S_{NO,\mathrm{het},rebur} = r_{het,rebur} M_{NO} 10^{-3} \tag{30}$$

The rate of heterogeneous reduction of NO on the char surface, $r_{het,rebur}$, is modelled according to Levy et al. [71]; $S_{NO,hom,rebur}$ is the source term due to homogenous re-burning and the rates constants are taken from [49]:

$$S_{NO,hom,rebur} = -(r_{hom,rebur,1} + r_{hom,rebur,2}) M_{NO} 10^{-3} \tag{31}$$

In this work, it is assumed that the re-burning agent is the volatile specie ($C_{1.33}H_{4.13}O_{0.50}$).

3. NUMERICAL APPROACH

The commercial code ANSYS FLUENT [49] is used to perform the numerical simulations. The presence of coal particles dispersed in the continuous gas phase is modeled by adopting a Lagrangian reference frame; the Discrete Phase Model, in particular, is used to compute the particles trajectories. Turbulence in the continuous phase is modeled using the standard k-ε model, with a wall function approach. Table 3 summarizes the models adopted for current simulations. More details regarding the settings for sub-models as well as the initial and boundary conditions are reported in the next sections.

The equations are discretized in space by adopting a cell-centered finite volume technique; a pressure-based algorithm is used to solve the discretized equations sequentially and the PISO pressure-velocity coupling is adopted to enforce mass conservation, resulting in a pressure correction equation. Second-order upwind schemes and second-order central differences are employed for discretization of convective and diffusion terms, respectively.

The proposed model was widely validated in [72], where simulations of MILD combustion in a pilot furnace and the comparison with experimental data are presented. This modeling approach was used to simulate Oxy-MILD combustion in the same pilot furnace and results showed that nitric oxides emissions were reduced by about 20% when compared to MILD combustion.

The main purpose of the present work is the evaluation of the possibility of taking advantage of Oxy-MILD combustion in a new concept of industrial boiler [38].

3.1 Geometry

An industrial boiler, with a high degree of internal recirculation, is analyzed in order to investigate the possibility of obtaining MILD combustion under Oxy-combustion condition. The geometry is the one proposed by Schaffel et al. [38], who introduced an innovative concept of boiler. The shape of the boiler is shown in Fig.2. The boiler is 13m high and is equipped with five burners, which are located at the top wall of the boiler, while the outlets of combustion products are set on the side of it. In this way, boiler internal gases recirculation is intensified. Each burner is composed of a central jet of coal and six O_2/CO_2 mixture jets localized along a circumference with a radius of 0.5m. A little part of carbon dioxide is used as a primary jet for coal transportation. Differently from [38], the FLOX (Flameless Oxidation) burner type is adopted in the current simulations. The computational domain is discretized by using a

structured mesh. It consists of about 1.0M cells and is refined in proximity of the burner. Figure 3 shows the computational domain of the top wall.

3.2 Test conditions and settings

A O_2/CO_2 mixture, with 33% oxygen and 67% carbon dioxide concentration without flue gas recycle (RFG) is used in the present work. Three excess oxygen ratios λ=1, λ=1.05, λ=1.1 (reference case) are analyzed. However, in order avoid aerodynamic effects, the oxygen, carbon dioxide and the transport carbon dioxide supplied at the burner are kept at a constant volume flow rate; therefore, the excess oxygen ratio changes with the coal flow rate. The thermal load, for the three cases, ranges from 133 to 143 MW_{th}. The operational condition for the three cases are summarized in Table 4.

The boundary conditions adopted for the analysis of the Oxy-MILD combustion in the new-concept boiler for the reference case are summarized in Table 5.

The CPD model parameters obtained by Genetti correlation (Eq.9), are listed in Table 6.

3.3 Grid dependence study

A grid dependence study with three different meshes is presented. The value of temperature at the boiler exit is used as a key parameter to evaluate the grid convergence, for the test condition described in section 3.2, for the reference case (λ=1.1). The approach adopted in this work is the one proposed by Stern et al. [73]. The mesh refinement ratio for grid convergence study is $\sqrt{2}$, therefore the grids dimensions for G1, G2 and G3 are 1.4, 1.0 and 0.71M, respectively.

The convergence ratio is defined as:

$$R = \frac{S_2 - S_1}{S_3 - S_2} \tag{32}$$

where S_1, S_2 and S_3 are the solutions corresponding to the fine, medium and coarse grid, respectively. When monotonic convergence is achieved, (0<R<1), the generalized Richardson extrapolation is used for the estimation of numerical errors and uncertainties. When solutions are in the asymptotic range (i.e. the mesh becomes "small" and asymptotically "close to zero"), numerical errors are evaluated according to the following formulation:

$$\delta_{RE} = \frac{\varepsilon_{21}}{r^p - 1} \tag{33}$$

where $\varepsilon_{21} = S_2 - S_1$, r is the refinement ratio and p is the estimated order of accuracy, calculated as:

$$p = \frac{ln[(S_3 - S_2)/(S_2 - S_1)]}{ln(r)} \tag{34}$$

and the uncertainty $U_G=0$. However, practically the asymptotic range is rarely achieved; in such cases, a corrected approach can be adopted for the estimation of numerical uncertainties [73]. Eq. 33 is corrected through a multiplication factor, C_G, which takes into account the effects of higher-order terms and provides a quantitative metric to determine the proximity of the solutions to the asymptotic range:

$$C_k = \frac{r^p - 1}{r^{pest} - 1} \tag{35}$$

$$\delta^* = C_G \delta^*_{RE} = C_G \frac{\varepsilon_{21}}{r^p - 1} \tag{36}$$

p_{est} in Eq.35 is the theoretical order of accuracy. When solutions are far from the asymptotic range, C_G is sufficiently less than or greater than 1 and only the magnitude of the error is estimated through the uncertainty U_G:

$$U_G = \left|C_G \delta^*_{G,RE}\right| + \left|(1 - C_G)\delta^*_{G,RE}\right| \tag{37}$$

When solutions are close to the asymptotic range, C_G is close to 1 and U_G is estimated by:

$$U_G = \left|(1 - C_G)\delta^*_{G,RE}\right| \tag{38}$$

Table 7 summarizes the results of the grid convergence study. Monotonic convergence is achieved by increasing the mesh quality. The results show that the solution is far from the asymptotic range ($C_G=0.33$), therefore Eq. 37 is used to determine grid uncertainty. The results variation between the three grids is negligible; in particular, the difference between S_1 and S_2

is not high enough to justify the use of the finest mesh and grid uncertainty, U_G, amounts to about 0.05% S_1. Consequently, the medium grid G_2 is a good compromise between solution accuracy and computational effort and the refinement level adopted in the medium mesh can be considered satisfactory for results reliability.

4. RESULTS AND DISCUSSION

4.1 Temperature, oxygen and carbon dioxide concentrations

This section presents the results for the industrial boiler, which operates under conditions reported in Table 5.

Fig. 4 reports the temperature, oxygen concentration and carbon dioxide fields in the whole boiler for the reference case (λ=1.1). Overall, the distributions are quite uniform, owing to the large volume of the boiler, which allows a better recirculation of combustion products; the pulverized coal meets and entrains a large amount of flue gas and can burn in a diluted environment; the devolatilization is very fast and the ignition occurs in proximity of the burner. In particular, the distributions are very uniform in the zone of the boiler close to the outer walls. In order to evaluate the uniformity of the temperature distribution quantitatively, statistical parameters such as standard deviation, skewness and kurtosis were calculated over the whole volume of the boiler. Table 8 shows that the standard deviation value of temperature is 95, while skewness and kurtosis are 0.006 and 0, respectively. The uniformity of temperature distribution is good and the value of standard deviation differs from the value found by Schaffel [38], where a standard deviation amounting to 250 was obtained. Furthermore, the distribution is symmetric (skewness = 0.006) and it assumes a Mesokurtic distribution (kurtosis = 0) [74].

More consistent variations occur along the height of the boiler, where the average temperature and carbon dioxide concentrations increase while the oxygen concentration decreases, owing to the enhancement of combustion intensity. This aspect is better highlighted in Fig. 5, where the oxygen, the carbon dioxide concentrations and the temperature profiles are shown in four cross-sections located at 2m, 4m, 6m and 8m from the burners. The profiles are taken along the *x*-axis, where the coordinates (*x=0, y=0.5) (see Fig.2)* correspond to O_2/CO_2 jet of a single burner. For each section, the profiles are quite uniform in the external region of the boiler. Moreover, downstream of section 3, the profiles are uniform along the whole axis. The average and peak temperatures in the boiler are 1495 K and 1880 K, respectively, while at

the boiler exit it is about 1393 K. The carbon dioxide at the boiler outlet is about 95.8%, the oxygen concentration amounts to 3.7% and char burnout is 99.3%.

The results for different excess oxygen ratios are simulated and summarized in Table 9, which reports the oxygen, carbon dioxide concentrations at the outlet of the boiler and char conversion. The oxygen concentration at the outlet, in the boiler operated at λ=1, is lower ([O_2] =0.8%) than in the boiler operated at λ=1.05 ([O_2]=2.5%) and λ=1.1 ([O_2]=3.7%), as expected. The computed values are affected by the uncertainties related to numerical and modeling errors. However, the oxygen concentration trend with increasing the oxygen excess is well caught. In particular, it is worth noting that, for stoichiometric combustion, some oxygen excess is obtained at the boiler exit: this is mainly due to the incomplete combustion, (char conversion ~98%). The char conversion diminishes as the excess oxygen ratio decreases, resulting in an incomplete combustion (carbon monoxide in the exhaust gases and carbon in ash). On the other hand, a too high oxygen excess involves a higher amount of nitric oxides at the outlet. This last aspect will be better discussed in section 4.2.

The recirculation in the boiler, for the reference case, is shown in Fig.6, which displays the axial velocity contours: almost the whole volume of the boiler is characterized by a strong recirculation, the combustion products rise toward the top of the boiler and the recirculation intensity is greater in the external part of it. Owing to the strong recirculation, which occurs in the boiler, a uniform distribution of heat flux at the wall is obtained, as displayed in Fig.7. Uniformity of radiative heat flux is desirable in order to improve the efficiency of the heat transfer from the combustion products to the water/steam mixture inside the tubes of a boiler in once-through configuration water circulation.

The average heat flux obtained in the current simulations under oxy-MILD conditions is shown in Fig.8. For the sake of comparison, the heat flux obtained under MILD conditions [38] and typical heat flux profiles for fluidized bed boilers and conventional wall-fired boilers [75] are also shown. The most relevant finding is that Oxy-MILD combustion maintains the heat flux uniformity, which is typical of combustion under MILD conditions and of combustion in fluidized bed boilers. In the current simulations, in particular, the heat flux value is comparable with the fluidized bed one; however, higher heat fluxes, typical of conventional boilers (250÷350 kW/m^2), can be obtained by modifying the operating conditions, i.e. inlet oxidizer temperature, oxygen excess ratio.

4.2 NO_x concentrations

The net fuel-NO_x formation in a combustion process is a balance between the HCN released by volatiles and char, by the level of oxygen in combustion chamber and by the re-burning path. This mechanism is plotted in Fig.9, which shows the numerical results of Fuel-NO_x, HCN concentrations and molar re-burning rate in the longitudinal section of the boiler are plotted. The HCN concentration is maximum in the coal injection zone (Fig.9, middle), owing to the coal devolatilization process. In the injection coal zone, no NO_x formation occurs (Fig.9, top) owing to the lack of oxygen. The NO_x starts to form in an intermediate zone between the coal jet and the O_2/CO_2 jet, according to the mechanism described by Eq. 19.a. Simultaneously, a rapid re-burning (Fig.9, bottom), occurring in the region between the volatiles release and the O_2/CO_2 jet, facilitates the destruction of the fuel-NO_x, according to Eq. 20. Owing to this mechanism, NO_x emissions are reduced primarily in proximity of the O_2/CO_2 jets near the burner and no NO_x is present in this zone. In the lower region of the boiler, the presence of NO_x is justified by the occurrence of transport phenomena; in this region, in fact, no char and no volatiles are present.

Fig. 10 displays the fuel-NO_x and oxygen concentrations profiles for the three different operating conditions in four cross-sections located at 2m and 4m from the burners. The profiles are obtained in the *zy*-symmetry plane, for half boiler length in the *y* direction; *y=2* corresponds to the central burner coal inlet. For all cases, the peak of NO_x is located in the region between the coal jet and the O_2/CO_2 one and no NO_x formation takes place in the coal jet. The operating condition λ=1, as expected, provides a lower amount of NO_x due to lower values of oxygen concentration. On the contrary, as the excess oxygen ratio increases, the NO_x increases as well. This aspect is better shown in Fig. 11, which reports the Fuel-N conversion ratio for the three operating conditions. Fuel-N conversion ratio, calculated according to Tu et al. [45] allows the Fuel-N conversion to be characterized. The results found in the present work are in accordance with the literature [20, 76, 77].

Fuel-NO_x concentration at the boiler exit is summarized in Table 10 under different excess oxygen ratios. The cases at λ=1.1 and λ=1.05 provide values close to the European legislation limit, 500 mg/Nm^3 @6%O_2; the case λ=1 provides a value considerably lower than this limit. However all cases are lower than typical emission values of standard PC burners (600-800 mg/Nm^3 [78]). Despite the case λ=1 appearing to be the best operating condition for NO_x

emissions, it provides a lower char conversion than the other cases. In order to emphasize the advantages of the oxy-MILD combustion in terms of NO_X reductions for the operating conditions analyzed in the present work, a comparison with other technologies is carried out and results are summarized in Table 11. For a neutral comparison between the different technologies, it is appropriate to use the emission rates [mg/MJ]. NO_X emission rates for conventional PC combustion in air are obtained from experiments carried out in pilot and lab scales and they range between 220÷350 mg/MJ [10,77,79-82]. Lower NO_X emission intensities (up to 70÷80% lower) are obtained under oxy conditions both for the absence of thermal NO_X, and for the re-burning of NO in the recycled flue gas [4, 77, 79-82]. By considering MILD technology, in the study proposed by Schaffel [38], a significant reduction amounting to 60÷80%, is achieved if compared to conventional coal combustion technology. They explain this reduction by considering that fuel-N is converted to molecular nitrogen rather than to NO, owing to a highly sub-stoichiometric condition in proximity of the devolatilization region. In addition, there are stronger NO-re-burning mechanisms and lower temperatures (1600÷2000K) under MILD conditions. In the current work, where MILD and oxy conditions are combined together, an even lower value of NO_X emission intensity than MILD (~40% lower) is achieved; this value is, however, comparable with oxy combustion even though in the present case no flue gas recirculation is considered. The results indicate that MILD condition makes the major contribution to the reduction of NO_X intensity; a further decrease with respect to MILD can be, however, achieved by considering that under oxy combustion thermal NO_X are absent. Moreover, in the current simulations, the lower temperatures (1400÷1800 K), the slightly lower oxygen concentration and the lower excess oxygen ratio than MILD also contribute to NOx reduction.

In order to emphasize the role of re-burning mechanism on NO_x emissions, a comparison with NO recirculation is considered and results are summarized in Table 12. An amount of about 150 ppmvd of recycled NO at inlet are considered. The overall fuel NO production rate is $14.5 \cdot 10^{-4}\ kg_{NO}/s$ and the NO reburning rate amounts to $5.5 \cdot 10^{-4}\ kg_{NO}/s$. Therefore, the net NO production rate in the boiler is $9 \cdot 10^{-4}\ kg_{NO}/s$. This value is exactly the difference between the amount of the NO at the exit ($17 \cdot 10^{-4}\ kg_{NO}/s$) and the one of the inlet ($8 \cdot 10^{-4}\ kg_{NO}/s$). The NO re-burning rate is about 38 % of the fuel-NO rate, which proves that this mechanism plays an important role in Oxy-MILD combustion, especially when recycled NO_x is considered. Under this condition, the NO emission rate at the outlet amounts to 45

mg/MJ if a 40% by mass of the flue gas is recycled. In the case where no recycle occurs, the NO re-burning rate is about 20% of the fuel-NO rate. In summary, with a recirculation, the re-burning rate increases from 20% to 38% and a reduction in NO_X emission rate from 70 to 45 mg/MJ seems to occur.

5. SUMMARY AND CONCLUSIONS

In this work, the possibility of exploiting the advantages of MILD combustion and Oxy combustion in pulverized coal-fired power plants was investigated by the use of CFD. The effective potential of Oxy-MILD combustion and its possible applications on an industrial scale are presented.

Results show that the temperature and species concentration distributions reach an acceptable level of uniformity in the boiler; similarly, the wall heat flux profile is uniform along the boiler height and is comparable with the ones of a fluidized bed boiler.

The predicted carbon dioxide concentration at the boiler outlet, for the reference case λ=1.1 is about 95.8%; this quantity slightly increases if the excess oxygen ratio is reduced to λ=1, even though incomplete combustion occurs.

A model for predicting NO_x emissions is also considered. The numerical results show that Oxy-MILD combustion could be an important technology for the reduction of nitric oxides when compared to conventional technology. This is due to the absence of N_2 in the oxidizer, which prevents the thermal and prompt NO_x, and to the strong recirculation, which favors the NO_x re-burning route. This mechanism appears to be the dominant reduction mechanism under oxy-MILD conditions and gives an even more important contribution when recycled NO occurs.

This study constitutes an early stage in the investigation of Oxy-MILD combustion; the presented results show the great potential of the Oxy-MILD combustion of pulverized coal in boilers in term of performance and environmental impact, and underline the critical aspects of boiler geometry. Future work will consist in the optimization of the geometry and of the velocity of the oxygen jet and in the analysis of using different low rank coals.

REFERENCES

[1] International Energy Agency, World Energy Outlook 2011, IEA, 696 p, ISBN: 978 92 64 12413 4, November 2011.

[2] EIA, U.S. Energy Information Administration, International Energy Outlook 2011, DOE/EIA0484, 2011.

[3] BP p.l.c., BPs Energy Outlook 2030, January 2013.

[4] Chen, L., Yong, SZ, Ghoniem AF., "Oxy-fuel combustion of pulverized coal: Characterization, fundamentals, stabilization and CFD modeling", Progress in Energy and Combustion Science, 2012; 38(2):156-214.

[5] Horn, F.L., Steinberg, M., "Control of carbon dioxide emissions from a power plant (and use in enhanced oil recovery)", Fuel, 1982;61:415-22.

[6] Abraham, B., Asbury, J., Lynch, E, Teotia, A., "Coal-oxygen process provides carbon dioxide for enhanced recovery", Oil Gas Journal,1982; 80:68-70.

[7] Steinberg, M., "History of CO_2 greenhouse gas mitigation technologies", Energy Conversion and Management, 1992;33:311-5.

[8] Wang, C.S., Berry, G.F., Chang, K.C., Wolsky, A.M. "Combustion of pulverized coal using waste carbon dioxide and oxygen", Combust Flame, 1988;72(3):301-10.

[9] Payne, R., Chen, S.L., Wolsky, A.M., Richter, W.F., "CO_2 recovery via coal combustion in mixtures of oxygen and recycled flue gas", Combust Sci Technol, 1989;67(1):1e16.

[10] Woycenko, D.M., van de Kamp, W.L., Roberts, P,A. "Combustion of pulverised coal in a mixture of oxygen and recycled flue gas", Summary of the APG research program, IFRF Doc. F98/Y/4. Ijmuiden, The Netherlands: International Flame Research Foundation (IFRF); October 1995.

[11] Tan, R., Corragio, G., Santos, S., "Oxy-coal combustion with flue gas recycle for the power generation industry e a literature review", Study report, IFRF Doc. No. G 23/y/1. Velsen Noord, The Netherlands: International Flame Research Foundation (IFRF); September 2005.

[12] Khare, S.P., Wall, T.F., Farida, A.Z., Liu, Y., Moghtaderi, B., Gupta, R.P., "Factors influencing the ignition of flames from air-fired swirl pf burners retrofitted to oxyfuel", Fuel, 2008;87(7):1042-9.

[13] Wall, T., Liu, Y., Spero, C., Elliott, L., Khare, S., Rathnam, R., et al, "An overview on oxyfuel coal combustion and State of the art research and technology development", Chem Eng Res Des, 2009;87(8):1003-16.

[14] Wall, T.F., “Performance of PF boilers retrofitted with oxy-coal combustion: understanding burnout, coal reactivity, burner operation, and furnace heat transfer” In: 3rd Workshop of the IEA GHG international oxy-combustion network. Yokohama, Japan; March 5-6, 2008.

[15] Toftegaard, M.B., Brix, J., Jensen, P.A., Glarborg, P., Jensen, A.D., “Oxy-fuel combustion of solid fuels”, Progress in Energy and Combustion Science, 2010;36:581-625.

[16] Li, H., Yan, J., Yan, J., Anheden, M., “Impurity impacts on the purification process in oxy-fuel combustion based CO_2 capture and storage system”, Appl Energy, 2009; 86:202–13.

[17] Hu, Y., Yan, J., “Characterization of flue gas in oxy-coal combustion processes for CO_2 capture”, Appl Energy, 2012; 90:113–21.

[18] Hu, Y., Yan, J., Li, H., “Effects of flue gas recycle on oxy-coal power generation system”, Appl Energy, 2012; 97:255–63.

[19] Hu, Y.,-Yan, J. “Numerical simulation of radiation intensity of oxy-coal combustion with flue gas recirculation”, Int J Greenhouse Gas Control, 2013; 17: 473–80.

[20] Álvarez, L., Gharebaghi, M., Jones, JM., Pourkashanian, M., Williams, A., Riaza, J., et al. “CFD modeling of oxy-coal combustion: prediction of burnout, volatile and NO precursors release”, Appl Energy, 2013; 104:653–65.

[21] Álvarez, L., Yin, C., Riaza, J., Pevida, C., Pis, JJ., Rubiera, F. “Oxy-coal combustion in an entrained flow reactor: Application of specific char and volatile combustion and radiation models for oxy-firing conditions”, Energy, 2013; 62:255–68.

[22] Hu, Y., Li, HL., Yan, JY. “Numerical investigation of heat transfer characteristics in utility boilers of oxy-coal combustion,”Appl Energy, 2014; 130:543–51.

[23] Okazaki, K., Ando, T. “NO_x reduction mechanism in coal combustion with recycled CO_2”, Energy, 1997; 22:207-215.

[24] Ikeda, M., Toporov, D., Christ, D., Stadler, H., Foerster, M., Kneer, R. “Trends in NO_x emission during pulverized fuel oxy-fuel combustion”, Energy Fuels, 2012; 26 (6): 3141–3149.

[25] Kawai, K.,Yoshikawa, K., Kobayashi, H., Tsai, JS., Matsuo, M., Katsushima, H. “High temperature air combustion boiler for low BTU gas”, Energy Convers Manag, 2002; 43:1563-70.

[26] Zhang, H., Yue, G., Lu, J., Jia, Z., Mao, J., Fujimori, T. et al. “Development of high temperature air combustion technology in pulverized fossil fuel fired boilers”. Proc Combust Inst, 2007; 31:2779- 85.

[27] Schaffel, N., Mancini, M., Szlek, A., Weber, R. “Mathematical modeling of MILD combustion of pulverized coal” Combust Flame, 2009;156:1771-84.

[28] Katsuki, M., Hasegawa, T. “The science and technology of combustion in highly preheated air”, Proc. Combust. Inst., 1998; 27:3135–3146.

[29] Wünning, J.A., Wünning, J.G. “Flameless oxidation to reduce thermal NO-formation”, Prog. Energy Combust. Sci., 1997; 23:81–94.

[30] Arghode, V.K., Gupta, A.K., Bryden, K.M. “High intensity colorless distributed combustion for ultra low emissions and enhanced performance”, Appl. Energy, 2012; 92:822–830.

[31] Li, P., Mi, J., Dally, B., Wang, F., Wang, L., Liu, Z., et al. “Progress and recent trend in MILD combustion”, Sci China Technol Sci, 2011; 54:255-69.

[32] Mi, J., Li, P., Dally, B.B., Craig, R.A. “Importance of initial momentum rate and air-fuel premixing on moderate or intense low oxygen dilution (MILD) combustion in a recuperative furnace”, Energy & Fuels, 2009; 23:5349-56.

[33] Weber, R., Verlaan, A., Orsino, S., Lallemant, N. “On emerging furnace design methodology that provides substantial energy savings and drastic reductions in CO_2, CO and NO_x emissions”, J. Inst. Energy, 1999; 72:77-83.

[34] Weber, R., Verlaan, A., Orsino, S., Lallemant, N. “Combustion of natural gas with high temperature air and large quantities of flue gas,” Proc. Combust. Inst., 2000, 28:1315-1321.

[35] Suda, T., Tajafuji, M., Hirata, T., Stato, J. “A study of combustion behavior of pulverized coal,” Fuel, 2004; 83: 1133-1141.

[36] Ristic, D., Schuster, A., Scheffknecht, G., Stadler, H., Foerster, M., Kneer, R., Wunning, JG. “Experimental study on flameless oxidation of pulverized coal in bench and pilot scale,” Proceeding of the 23th German Flame day, Berlin, Germany, 2007.

[37] Ristic, D., Schuster, A., Scheffknecht, G., Stadler, H., Foerster, M., Kneer, R., Wunning, JG. “Investigation of NO_x formation for flameless coal combustion,” Proceedings of the 7th HiTACG Symposium, Phuket, Thailand, 2008.

[38] Schaffel, N., Mancini, M., Szlek, A., Weber, R. “Novel Conceptual Design of a Supercritical Pulverized Coal Boiler Utilizing High Temperature Air Combustion (HTAC) Technology”, Energy, 2010; 35:2752-2760.

[39] Perrone, D., Amelio, M. “Numerical Simulation of MILD (Moderate or Intensive Low-oxygen Dilution) Combustion of Coal in a Furnace with different Coal Gun Positions”, International Journal of Heat and Technology, 2016; 34, 242-248

[40] Stadler, H., Ristic, D., Foerster, M., Schuster, A., Kneer, R., Scheffknecht, G. “NO_x-emissions from flameless coal combustion in air, Ar/O_2 and CO_2/O_2”, Proceedings of the Combustion Institute, 2009; 32:3131-3138.

[41] Seepana S, Jayanti S. “A new stable operating regime for oxyfuel combustion”, In: ASME international mechanical engineering congress and exposition. Boston, MA; 2008: 435-444.

[42] Calchetti G, Nardo AD, Mongibello G, Mongiello C., “Mild combustion simulation of coal water slurry”, In: Italian section of the combustion institute 30th meeting on combustion. Ischia, Italy; 2007.

[43] Li, P., Dally, B.B, Mi, J., Wang, F. “MILD oxy-combustion of gaseous fuels in laboratory-scale furnace”, Combustion and Flame, 2013; 160 (5) 933-946.

[44] Li, P., Wang, F., Tu, Y., Mei, Z., Zhang, J., Zheng, Y., Liu, H., Liu, Z., Mi, J. and Zheng C. “Moderate or Intense Low-Oxygen Dilution Oxy-combustion Characteristics of Light Oil and Pulverized Coal in a Pilot-Scale Furnace”, Energy & Fuels; 2014, 28 (2): 1524-1535.

[45] Tu, Y., Liu, H., Chen, S., Liu Z., Zhao, H., Zheng, C. “Numerical study of combustion characteristics for pulverized coal under oxy-mild operation,” Fuel Processing Technology, 2015, 135:80-90.

[46] Liu, R., An, E., Wu, K., Liu, Z. “Numerical simulation of oxy-coal MILD combustion with high-velocity oxygen jets”, Journal of the Energy Institute, 2017; 90:30-43.

[47] Hu, F., Li, P., Guo, J., Liu, Z., Wang, L., Mi, J., Dally, B., Zheng,C. “Global reaction mechanisms for MILD oxy-combustion of methane”, Energy, 2018; 147: 839-857.

[48] Adamczyk, W.P., Bialecki, R.A., Ditaranto, M., Gladysz, P., Haugen N.E.L., Katelbach-Wozniak, A., Klimanek, A., Sladek, S., Szlek, A., Wecel, G. “CFD modeling and thermodynamic analysis of a concept of a MILD-OXY combustion large scale pulverized coal boiler”, Energy, 2017; In-Press

[49] FLUENT Theory’s Guide- Fluent Inc. of ANSYS Inc.

[50] Fletcher, T.H., Kerstein, A.R., Pugmire, R.J., Solum, M.S., Grant, D.M. "Chemical percolation model for devolatilization: 3. Direct use of carbon-13 NMR data to predict effects of coal type", Energy and Fuels, 1992; 6: 414-431.

[51] Fletcher, T.H., Kerstein, A.R., Pugmire, R.J., Grant, D.M. "A chemical percolation model for devolatilization: 2. Temperature and heating rate effects on product yields", Energy and Fuels, 1990; 4:54-60.

[52] Flower, W.L, Hanson, R.K., Kruger, C.H., "Kinetics of the reaction of nitric oxide with hydrogen", Symposyum (International) on Combustion, 1975; 15:8232-832.

[53] Genetti, D., Fletcher, T.H., Pugmire, R. "Development and application of a correlation of C-13 NMR chemical structural analyses of coal based on elemental composition and volatile matter content", Energy and Fuels, 1999; 13 (1):60-8.

[54] Murphy, J., Shaddix, C., "Combustion kinetics of coal chars in oxygen-enriched environments", Combust Flame, 2006;144:710-29.

[55] Toporov D, Bocian P, Heil P, Kellermann A, Stadler H, Tschunko S, et al.,"Combustion kinetics of coal chars in oxygen-enriched environments", Combust Flame, 2008;155:605-18.

[56] Toporov, D., Bocian, P., Heil, P., Kellermann, A., Stadler, H., Tschunko, S., Förster, M., Kneer, R., "Detailed investigation of a pulverized fuel swirl flame in CO_2/O_2 atmosphere", Combustion and Flame, 2008, 155(4),pp.605-618

[57] Smith, T. F.; Shen, Z. F.; Friedman, J. N. J. Heat Transfer 1982, 104, 602–608.

[58] Yin, C., Johansen, L.C.R., Rosendahl L. A., Kaer, S. K., "New Weighted Sum of Gray Gases Model Applicable to Computational Fluid Dynamics (CFD) Modeling of Oxy-Fuel Combustion: Derivation, Validation, and Implementation", Energy&Fuels, 2010;24: 6275-6282.

[59] Ma, L., Gharebaghi, M., Porter, R., Pourkashanian, M., Jones, JM., Williams, A., "Modeling methods for co-fired pulverised fuel furnaces", Fuel, 2009;88:2448–54.

[60] Al-Abbas, A.H., Naser, J., Dodds, D., "CFD modeling of air-fired and oxy-fuel combustion of lignite in a 100 KW furnace", Fuel, 2011;90:1778–95.

[61] Álvarez, L., Gharebaghi, M., Pourkashanian, M., Williams, A., Riaza, J., Pevida, C., et al. "CFD modeling of oxy-coal combustion in an entrained flow reactor", Fuel Process Technol, 2011;92:1489–97.

[62] Zhang, J., Prationo, W., Zhang, L., Zhang, Z. “Computational fluid dynamics modeling on the air-firing and oxy-fuel combustion of dried Victorian brown coal”, Energy Fuels 2013;27:4258–69.

[63] Álvarez, L., Yin, C., Riaza, J., Pevida, C., Pis, J.J, Rubiera, F., “Biomass co-firing under oxy-fuel conditions: a computational fluid dynamics modeling study and experimental validation”, Fuel Process Technol, 2014;120:22–33.

[64] Yin, C., “On gas and particle radiation in pulverized fuel combustion furnaces”, Appl Energy, 2015;157:554–61.

[65] Lockwood, F.C., Rizvi, S.M., Shah, N.G., “Comparative predictive experience of coal firing”, Proceedings of the Institution of Mechanical Engineers, Part C: Journal of Mechanical Engineering Science, 1986;200:79-87.

[66] Yin, C., Yan, J., “Oxy-fuel combustion of pulverized fuels: Combustion fundamentals and modeling”, Applied Energy, 2016;162:742–762.

[67] Andersson, K., Johansson R., Hjärtstam S., Johnsson F., Leckner B., “Radiation intensity of lignite-fired oxy-fuel flames”, Experimental Thermal and Fluid Science, 2008;33:67-76

[68] He, R., Suda, T., Takafuji, M., Hirata, T., Sato, J., “Analysis of low NO emission in high temperature air combustion for pulverized coal”, Fuel, 2004; 83 (9): 1133–1141.

[69] Tu, Y., Liu, H., Chen, S., Liu, Z., Zhao, H., Zheng, C., “Numerical study of combustion characteristics for pulverized coal under oxy-MILD operation”, Fuel Processing Technology, 2015; 135: 80–90

[70] De Soete, G.G., “Overall Reaction Rates of NO and N_2 Formation from Fuel Nitrogen”, Proc. Combust. Inst., 1975; 15:1093‑1102,

[71] Levy, J. M.,. Chen, L. K, Sarofim, A. F., and Beer J. M., “NO/Char Reactions at Pulverized Coal Flame Conditions”, In 18th Symp. (Int’l.) on Combustion. The Combustion Institute. 1981.

[72] Perrone, D., Amelio, M. “Numerical investigation of oxy-mild combustion of pulverized coal in a pilot furnace”, Energy Procedia, 2016; 101:1191-1198.

[73] Stern, F., Wilson, R.V., Coleman, H.V., Paterson, E.G. “Comprehensive Approach to Verification and Validation of CFD Simulations—Part 1: Methodology and Procedures” Journal of Fluids Engineering, 2001, 123, pp0793-802.

[74] Westfall, P.H., Kurtosis as Peakedness, 1905 - 2014. R.I.P. The American Statistician 2014; 68,191-195.

[75] Lundquist, R., Schrief, A., Kinnunen. P., Myohanen, K., Seshamani, M. “A Major Forward - The Supercritical CFB Boiler”, In Power-Gen International 2003, Las Vegas, USA.

[76] Hu, Y., Naito, S., Kobayashi, N., Hasatani, M., “CO_2, NO_x and SO_2 emissions from the combustion of coal with high oxygen concentration gases” Fuel, 2000, 79(15),pp.1925-1932,

[77] Stadler, H., Christ, D., Habermehl, M., Heil, P., Kellermann, A., Ohliger, A., Toporov, D., Kneer, R., “Experimental investigation of NO_x emissions in oxycoal combustion”, 2011, Fuel, 90(4), pp. 1604-1611,

[78] Kakac, S., Boilers, evaporators and condensers. John Wiley & Sons, Inc., 1991.

[79] Nozaki, T., Takano, S., Kiga, T., Omata, K., Kimura, N. “Analysis of the flame formed during oxidation of pulverized coal by an O2/CO2 mixture”, Energy, 1997;22:199-205.

[80] Kimura, N., Omata, K., Kiga, T., Takano, S., Shikisima, S. “The characteristics of pulverized coal combustion in O2/CO2 mixtures for CO2 recovery”, Energy Conversion and Management, 1995;36:805-8

[81] Wall, T., Liu, Y., Spero, C., Elliott, L., Khare, S., Rathnam, R, et al., “An overview on oxyfuel coal combustion: State of the art research and technology development”, Chemical Engineering Research and Design, 2009;87:1003-16.

[82] Croiset, E., Thambimuthu, K.V., “NOx and SO2 emissions from O2/CO2 recycle coal combustion”, Fuel, 2001;80:2117-21.

[83] Verhoeff, F., Van Heek, P.H.G., “Two year operating experience with the AKZO 90MWth coal-fired AFBC boiler in Holland”, Proceedings of the 10th International Conference on FBC, San Francisco, 1989, Vol 1, pp. 289-296.

TABLES CAPTIONS

Table 1. Guasare coal proximate analysis [27].

Composition	Wt%
Moisture	2.9
Volatile Matter	37.1
Fixed carbon	56.7
Ash	3.3
LCV	31.74 MJ/kg

Table 2. Guasare coal ultimate analysis (dry, ash free basis) [27].

Composition	Coal	Char	Volatiles
C	81.6	92.6	72.51
H	5.5	1.3	9.10
N	1.5	1.7	1.3

O	10.7	4.0	16.3
S	0.6	0.4	0.8

Table 3. Sub-models used for coal combustion.

Physical process	Sub-model
Turbulence	Standard κ–ε model
Lagrangian particle tracking	Discrete Phase Model
Chemistry-Turbulence Interaction	Eddy Dissipation Model/Finite Rate Model (EDM/FRM)
Devolatilization	Chemical Percolation Devolatilization (CPD) Model
Char Combustion	Multiple particle surface reactions
Radiation	P-1 Model
NO_x model	Post-processing mode

Table 4. Operational Conditions.

CASES	λ	O_2 [%]	CO_2 [%]	Thermal Input [MWth]
1	1	33	67	143
2	1.05	33	67	137
3	1.1	33	67	133

Table 5. Boundary conditions for Oxy-MILD combustion for a quarter of boiler for the reference case (case 3)

	Type	Number	Settings
O_2/CO_2 Inlet	Velocity Inlet	10	O_2=33%; CO_2=67%; $\dot{m} = 8.2$ kg/s; v=120 m/s; T=850 K
Transport CO_2 Inlet	Velocity Inlet	3	%CO_2=100%; $\dot{m} = 0.2$ kg/s; v=30 m/s; T=300 K
Coal Inlet	Injection	3	$\dot{m} = 0.84$ kg/s; v=22.5 m/s; T=300 K
Outlet	Pressure Outlet	2	101325 Pa

Wall	Wall	-	T=800 K

Table 6. CPD model parameters.

Parameter	Symbol	Value	Unit
Cluster molecular weight	M_{cl}	359	kg/kmol
Side chain molecular weight	M_{del}	33.6	kg/kmol
Lattice coordination number	$\sigma+1$	4.95	-
Initial fraction of bridges in coal lattice	P_0	0.51	-
Initial fraction of char bridges	C_0	0	-

Table 7. Grid independence study for parameters at furnace exit.

Grid	N of cells [M]	Temp [K]	ε	R	C_G	δ_{RE}	U_G [% S_1]
G1	1.4	1392.7	0.7				
G2	1.0	1393.4	1.4	0.5	0.33	0.7	0.05
G3	0.71	1394.8					

Table 8. Statistical parameters for the reference case.

T_{ave} [K]	Standard Deviation	Skewness	Kurtosis
1495	95	0.006	0

Table 9. Oxygen, Carbon Dioxide Concentration and char conversion under different excess oxygen ratios.

λ	O_2 [% vol-dry]	CO_2 [% vol-dry]	Char Conv [%]
1	0.8	98.7	97.8
1.05	2.5	97.1	98.5
1.1	3.7	95.8	99.3

Table 10. NO_x emission at the exit under different excess oxygen ratios.

λ	NO_x @ 6% O_2[mg/Nm^3]
1	275
1.05	444
1.1	465

Table 11. Comparison of NOx emissions for different combustion technologies

	Oxidizer	λ	NOx (mg/MJ)
Combustion in air* [10,77,79-82]	air	1.15÷1.2	220÷350
Oxy combustion* [10,77,79-82]	O_2/CO_2 FGR (wet/dry)	0.8÷1.1	50÷200
MILD combustion† [38]	air	1.2	~135
Oxy-MILD combustion†	O_2/CO_2 (33%; 67%)	1.1	~70
Fluidized bed combustion* [83]	Air	1.2	50÷180

*From experiments in lab and pilot scale

† Calculated

Table 12. Mass balance of NO [kg_{NO}/s] with recycled NO for case 3.

	w NO recirculation	w/o NO recirculation
$\dot{m}_{NO.in}$	$8 \cdot 10^{-4}$	0
$\dot{m}_{NO.out}$	$-17 \cdot 10^{-4}$	$-15 \cdot 10^{-4}$
$\dot{m}_{NO.fuel}$	$14.5 \cdot 10^{-4}$	$20 \cdot 10^{-4}$
$\dot{m}_{NO.reburning}$	$-5.5 \cdot 10^{-4}$	$-5.0 \cdot 10^{-4}$
Reburning (%)	38%	20%

FIGURES CAPTIONS

Fig.1 NO_x formation and reduction mechanisms.

Fig.2 3D view (top), top view (bottom-left) and single burner (bottom-right) of the boiler.

Fig.3 Computational mesh boiler: top wall (left) and symmetry longitudinal plane (right).

Fig.4 Temperature field (top-left), oxygen concentration (top-right), carbon dioxide concentration (bottom-center).

Fig.5 Oxygen, carbon dioxide and temperature profiles along cross sections located at 2 m, 4 m, 6 m and 8 m from the burners.

Fig.6 Axial velocity contours.

Fig.7 Wall heat flux.

Fig.8 Average wall heat flux profile a) oxy-MILD; b) MILD [38]; c) fluidized bed [75]; d) conventional PC boiler [75].

Fig.9 Fuel NO concentration (top), HCN concentration (middle) and molar reburning rate (bottom) in the longitudinal plane.

Fig.10 Fuel NO profiles along cross sections located at 2m (top) and 4m (bottom), from the burners for different excess oxygen ratio values.

Fig.11 Fuel-N conversion ratio for different excess oxygen ratio values.

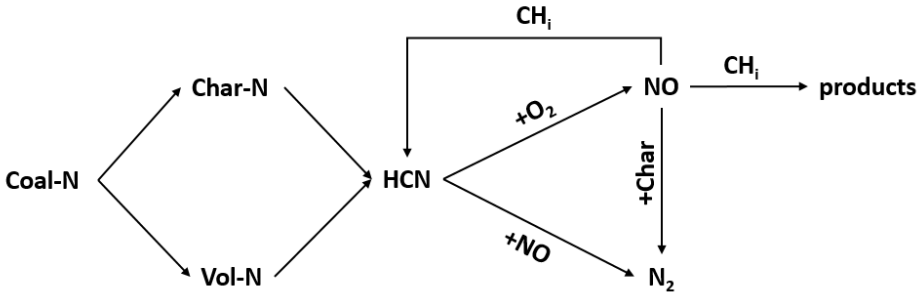

Fig.1 NO_x formation and reduction mechanisms.

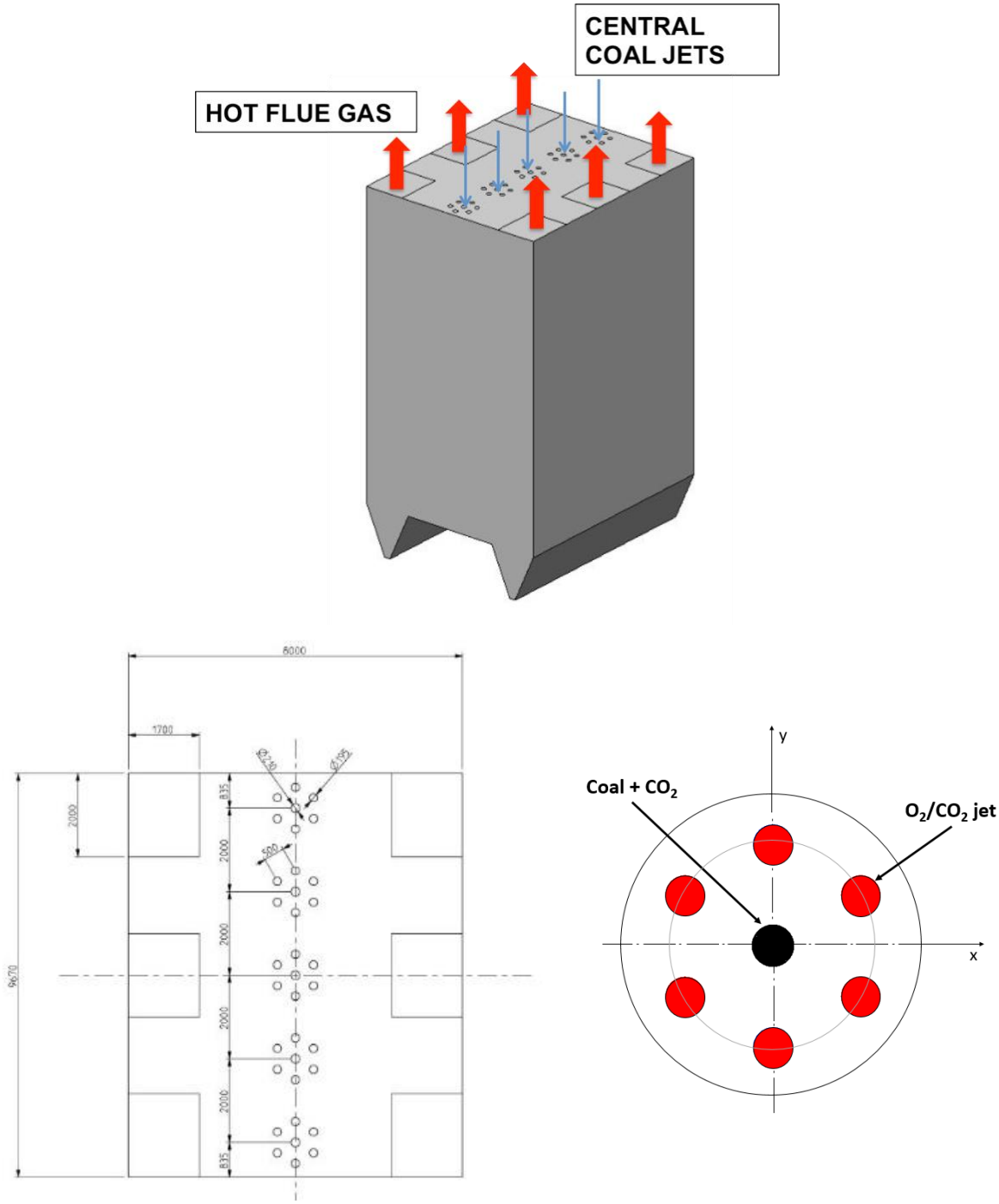

Fig.2 3D view (top), top view (bottom-left) and single burner (bottom-right) of the boiler.

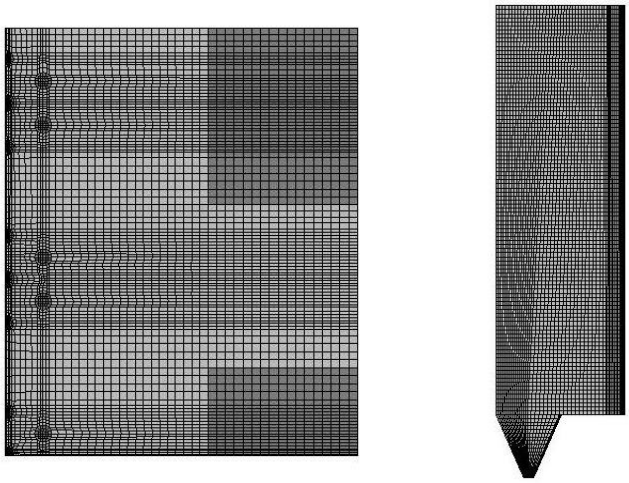

Fig.3 Computational mesh for boiler: top wall (left) and symmetry longitudinal plane (right).

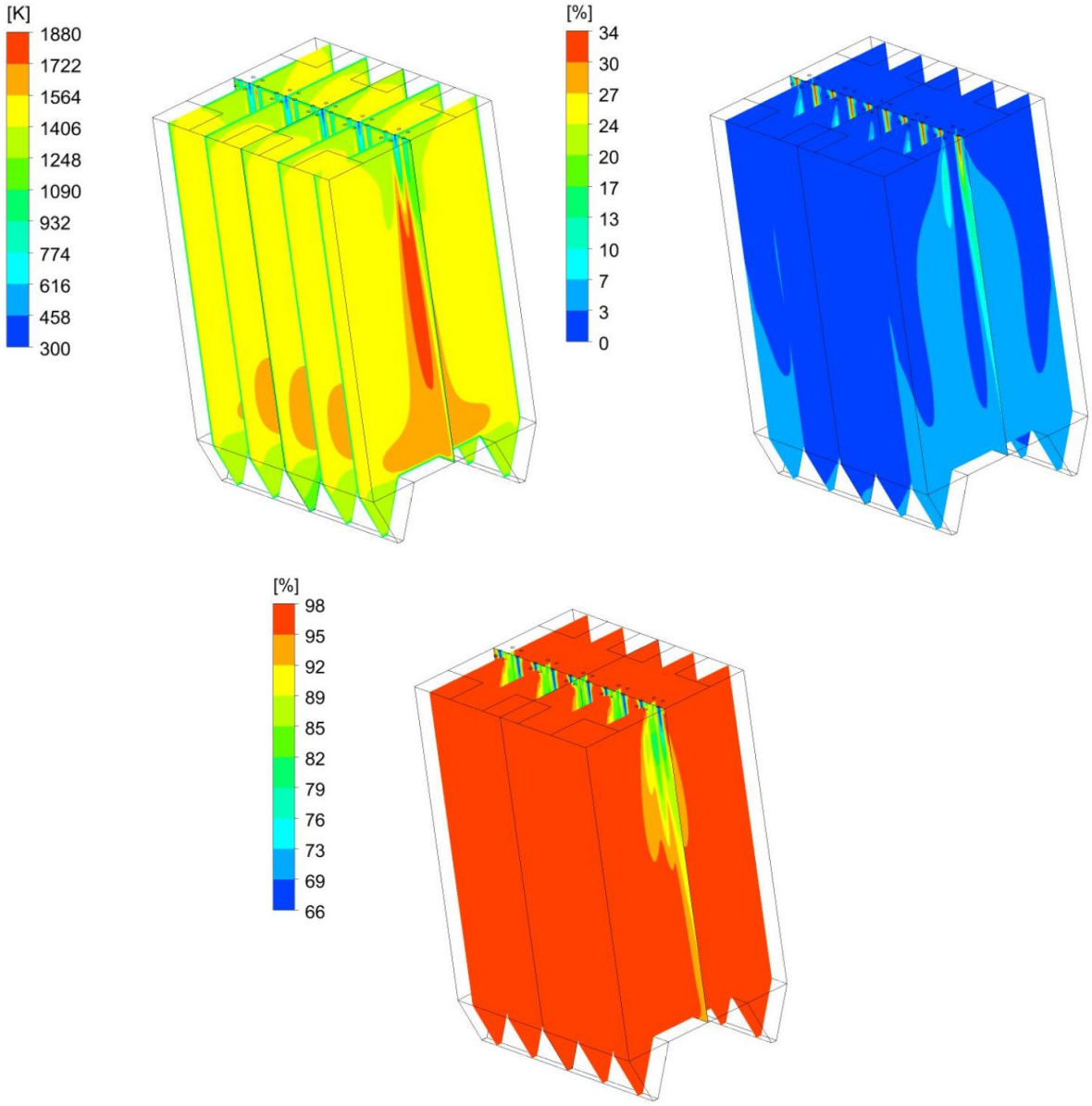

Fig.4 Temperature field (top-left), oxygen concentration (top-right), carbon dioxide concentration (bottom-center).

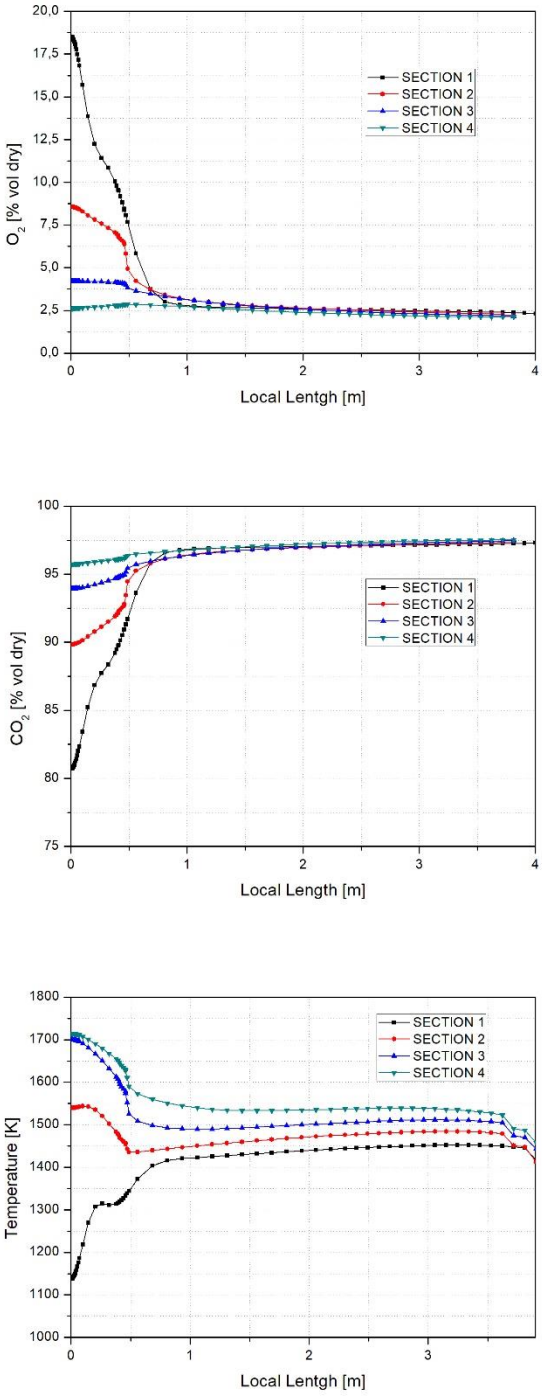

Fig.5 Oxygen, carbon dioxide and temperature profiles along four cross sections located at 2 m, 4 m, 6 m, and 8 m from the burners.

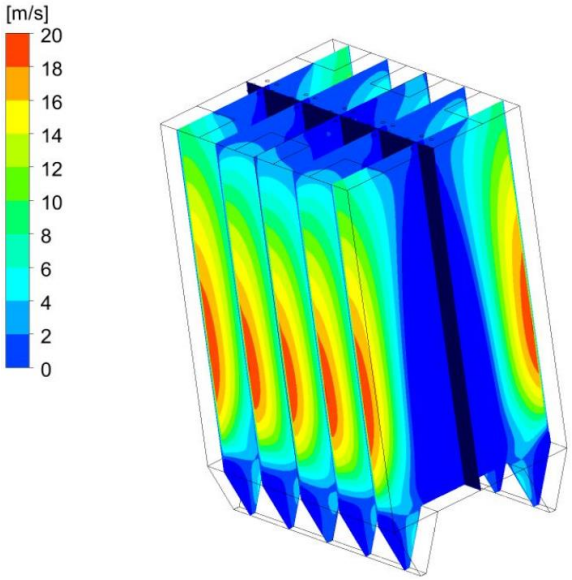

Fig.6 Axial velocity contours.

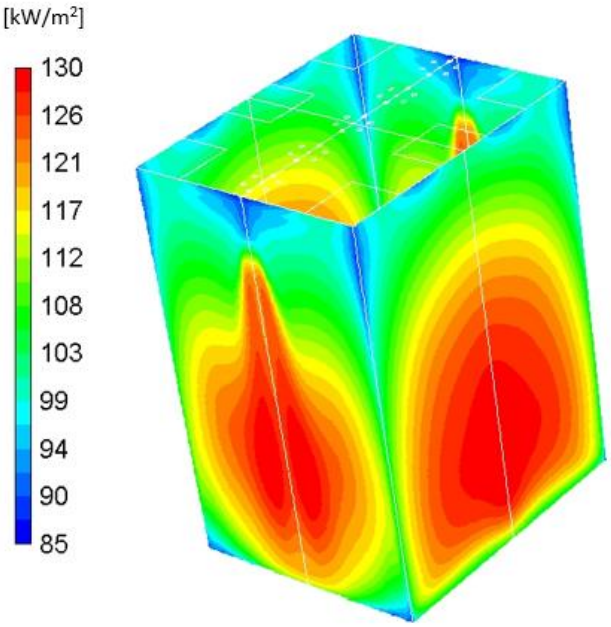

Fig.7 Wall heat flux.

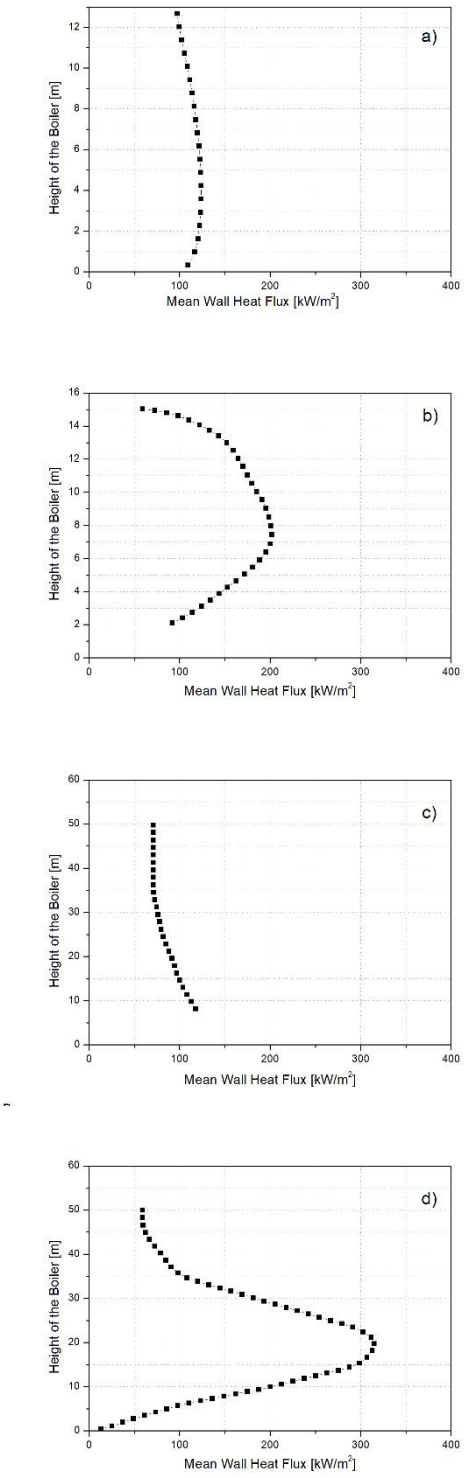

Fig.8 Average wall heat flux profile a) oxy-MILD; b) MILD [38]; c) fluidized bed [75]; d) conventional PC boiler [75].

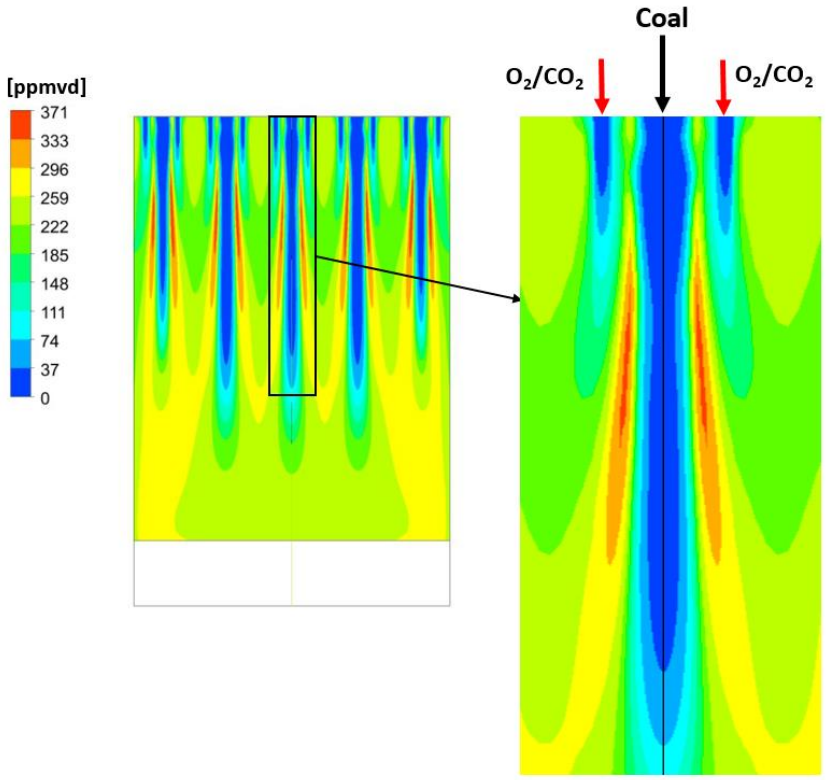
[ppmvd]
371
333
296
259
222
185
148
111
74
37
0
Coal
O2/CO2
O2/CO2

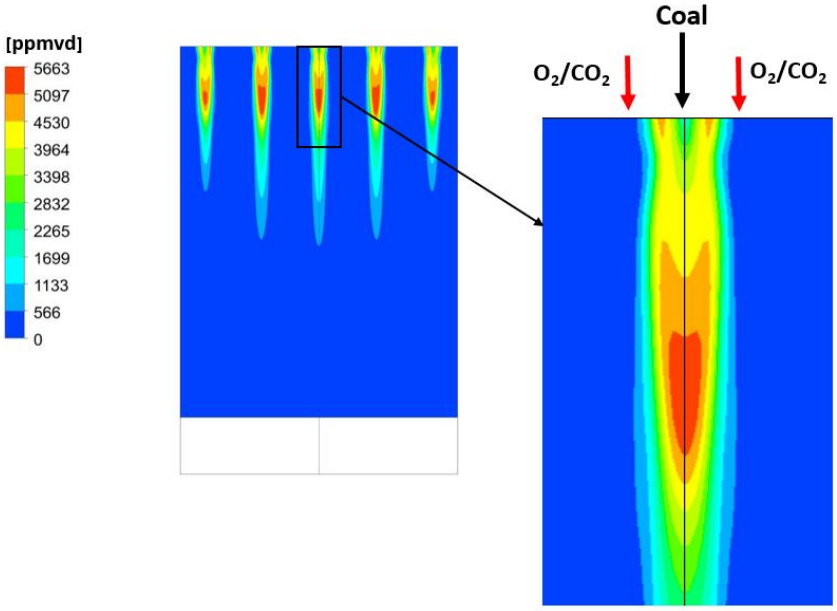
[ppmvd]
5663
5097
4530
3964
3398
2832
2265
1699
1133
566
0
Coal
O2/CO2
O2/CO2

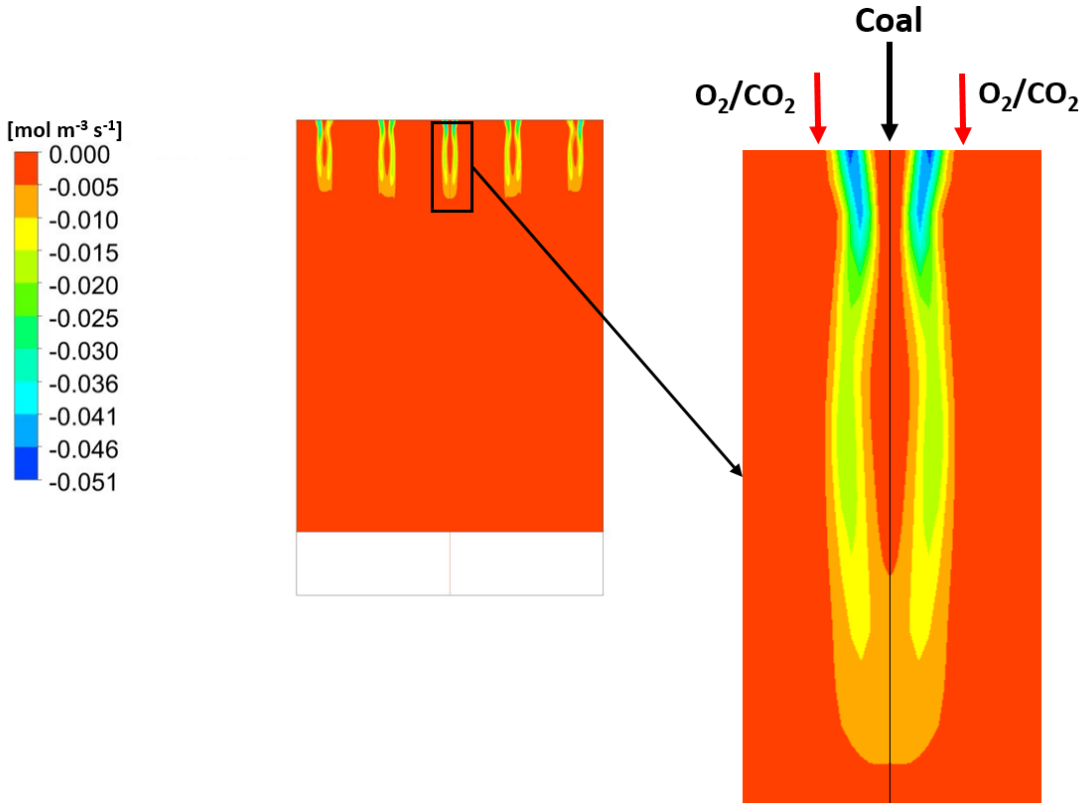

Fig.9 Fuel NO concentration (top), HCN concentration (middle) and molar reburning rate (bottom) in the longitudinal plane.

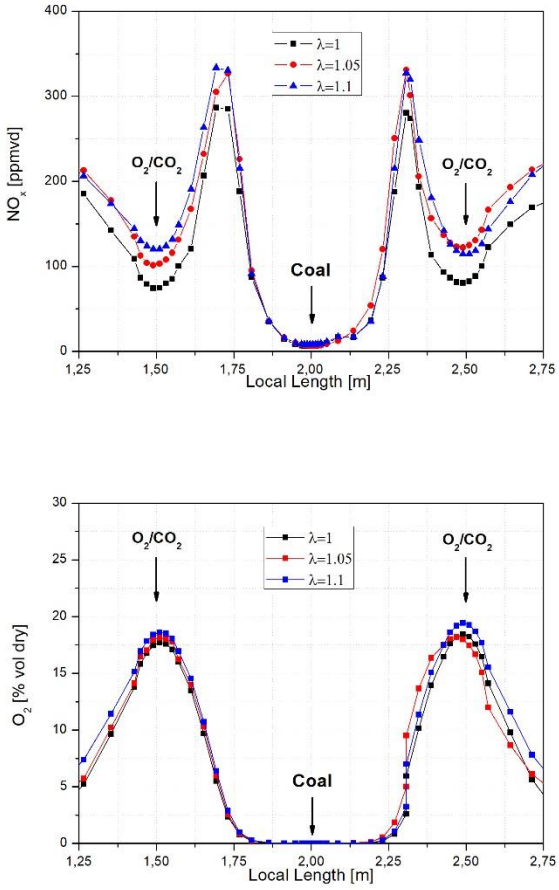

Fig.10 Fuel NO_x profiles along cross sections located at 2m (top) and 4m (bottom), from the burners for different excess oxygen ratio values.

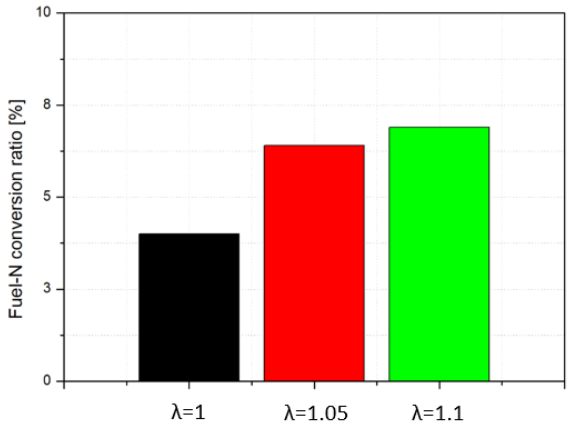

Fig.11 Fuel-N conversion ratio for different excess oxygen ratio values.